A Pulsar Wind Nebula in the Oxygen-Rich Supernova Remnant G292.0+1.8

John P. Hughes[1], Patrick O. Slane [2], David N. Burrows[3], Gordon Garmire[3], John A. Nousek[3], C. M. Olbert[4], and J. W. Keohane[4]

ABSTRACT

Using the *Chandra X-ray Observatory* we have discovered a diffuse, center-filled region of hard X-ray emission within the young, oxygen-rich supernova remnant (SNR) G292.0+1.8. Near the peak of this diffuse emission lies a point-like source of X-ray emission that is well described by an absorbed power-law spectrum with photon index 1.72 ± 0.09. This source appears to be marginally extended; its extent of $1.3''$ (FWHM) is greater than that of a nearby serendipitous X-ray source with FWHM = $1.1''$. This is strong evidence for the presence within SNR G292.0+1.8 of a young rapidly-rotating pulsar and its associated pulsar wind nebula. Both the X-ray and radio luminosity of the pulsar wind nebula imply a spin-down energy loss rate of $\dot{E} \sim 10^{37}\,\mathrm{ergs\,s^{-1}}$ for the still undetected pulsar. The pulsar candidate is $0.9'$ from the geometric center of the SNR which implies a transverse velocity of $\sim 770(D/4.8\,\mathrm{kpc})(t/1600\,\mathrm{yr})^{-1}\,\mathrm{km\,s^{-1}}$ assuming currently accepted values for the distance and age of G292.0+1.8.

Subject headings: ISM: individual (SNR G292.0+1.8, MSH 11−54) – pulsars: general – shock waves – supernova remnants – X-rays: ISM

1. Introduction

G292.0+1.8 (MSH 11−54) is a southern supernova remnant (SNR), discovered in the radio band (Milne 1969; Shaver & Goss 1970), with a radio spectral index intermediate

[1]Department of Physics and Astronomy, Rutgers University, 136 Frelinghuysen Road, Piscataway, NJ 08854-8109; jph@physics.rutgers.edu

[2]Harvard-Smithsonian Center for Astrophysics, 60 Garden Street, Cambridge, MA 02138; slane@head-cfa.harvard.edu

[3]Department of Astronomy & Astrophysics, 525 Davey Lab, Penn State University, University Park, PA 16802

[4]North Carolina School of Science and Mathematics, 1219 Broad St., Durham, NC 27705

between that of a typical shell-type and Crab-type remnant (Goss et al. 1979). Optically the spectrum is dominated by oxygen and neon emission lines (Goss et al. 1979) covering a wide range, $\sim$2000 km s^{-1}, in velocity (Murdin & Clark 1979). G292.0+1.8 is, therefore, an oxygen-rich SNR, of which there are only two other examples in the Galaxy (Cassiopeia A and Puppis A) and a handful elsewhere (e.g., N132D, E0540−69.3, and E0102.2−7219 in the Magellanic Clouds). It is believed that G292.0+1.8 is a young SNR with an age $\lesssim$ 1600 yr (Murdin & Clark 1979) in which the supernova ejecta have not yet fully mixed with the swept-up circumstellar material and thus may represent a slightly older version of Cas A.

Recent developments suggest that G292.0+1.8 is, in fact, a composite remnant, i.e., one showing both thermal emission from SN ejecta, as well as a synchrotron nebula powered by a rapidly rotating neutron star. Wallace & Gaensler (1997) presented a high resolution 20-cm radio map of the SNR from the Australia Telescope, which shows a bright, extended nebula near the center with a flatter spectrum ($\nu^{-0.4}$) than elsewhere in the remnant ($\nu^{-0.7}$). Pulsar-powered plerions, like the Crab Nebula, have traditionally been distinguished from their shell-type cousins by their flatter radio spectra. Recently Torii, Tsunemi, & Slane (1998) have reported on the G292.0+1.8 *ASCA* data. In addition to the thermal emission at soft X-ray energies, above $\sim$3 keV they found a hard X-ray source with a power-law spectrum, unresolved at *ASCA* angular resolution and positionally consistent (within the usual *ASCA* position uncertainty of 40″) with the extended, flat-spectrum radio component mentioned above. Although not conclusive, these observations suggest that a synchrotron nebula powered by the spin-down of a central pulsar possibly lurks within G292.0+1.8. This finding is quite important, since it would allow us to conclusively associate the young, oxygen-rich SNR G292.0+1.8 with a core-collapse, massive star SN explosion. Indeed only one other oxygen-rich remnant, SNR E0540−69.3 in the Large Magellanic Cloud, is known to contain a rapidly spinning pulsar.

2. Observations

G292.0+1.8 was observed with the back-side illuminated chip (S3) of the *Chandra* Advanced CCD Imaging Spectrometer (ACIS-S) (Garmire et al. 1992; Bautz et al. 1998) on 11 March, 2000, as part of the Penn State GTO program. Observations were taken in full frame mode with a readout time of 3.2 s. We filtered the data for times of flaring background or bad aspect solution, applied the bad pixel map, and verified that the level 2 events had been gain-corrected using the gain map appropriate to the focal plane temperature at the time of observation (−120° C). The effective deadtime-corrected exposure time after time filtering was 43026.6 s.

The S3 chip was used in order to take advantage of its soft response and good spectral resolution. The pointing direction was set so that as much of the remnant as possible fell on this chip. The remnant is slightly larger than $8'$ in diameter so complete coverage was not possible; small portions of the remnant toward the south and west were not imaged. In addition, we point out that the imaging quality varies across the S3 field of view. For this observation of G292.0+1.8 the aimpoint and its surrounding region of $1''$ imaging (50% encircled energy radius) is on the eastern half of the remnant. At the extreme northern and southern extent of the SNR, image quality has degraded to $\sim 1.5''$, while on the extreme western edge it has become $\sim 2.5''$.

3. Spectral and Spatial Analysis

In Figure 1 we show images of G292.0+1.8 in soft (left panel) and hard (right panel) X-ray bands. The soft X-ray image shows a highly structured and filamentary remnant with features on all scales from arcminutes to arcseconds. The brightest emission is mostly confined to an irregular "belt" that runs in an east-west direction across the remnant. These features tend to be quite narrow ($\lesssim 3''$) in the transverse (generally north-south) direction. Comparison of separate images made in energy bands containing the strong O, Ne, and Mg Kα lines reveals complex spectral variations with position. The integrated spectrum of the remnant (Figure 2) shows that lines from these species, in addition to Si and S, dominate the X-ray emission. Iron appears not to be a major constituent of the X-ray spectrum. There is no significant Fe K-shell emission: the equivalent width of a narrow line feature with energy between 6.4 and 6.9 keV in the integrated ACIS-S spectrum is <200 eV (at 95% confidence). We defer a more detailed quantitative discussion of the thermal emission from G292.0+1.8 to a future study.

In the higher energy band, we spectacularly confirm the previous radio and X-ray evidence for a plerion in G292.0+1.8. Embedded within a diffuse nebula approximately $1'$ in radius, we find a point-like source at position $\alpha_{\rm J2000} = 11^{\rm h}24^{\rm m}39.1^{\rm s}$, $\delta_{\rm J2000} = -59^\circ 16' 20.0''$, which we designate CXOU J112439.1$-$591620 (hereafter the "pulsar candidate"). We verified absolute positions in the ACIS image by identifying two serendipitous X-ray sources with optical stars ($m_R = 10$ and $m_R = 11.8$) from the USNO-A2.0 catalog. Our resulting X-ray positions are accurate to $<1''$.

Figure 3 shows a smoothed 4–8 keV X-ray image centered on the pulsar candidate. This band was chosen to isolate the hard nebular emission and represents a compromise between obtaining sufficient signal from the nebula and avoiding contamination by the generally softer thermal emission. The pulsar candidate, located near the peak of the diffuse emission, has a FWHM extent of $1.3''$, while the unrelated source nearby (which is at roughly the same off-axis angle) has an extent of $1.1''$, which we take to infer that the pulsar candidate has an extended component (perhaps a terminal wind boundary). (Neither source shows an obvious optical counterpart in the digitized POSS.) As the insert to Fig. 3 shows, the X-ray emission from the immediate vicinity of the pulsar candidate is rather complex with a symmetric, extended component (out to a radius of $\sim 1.5''$) embedded in a ridge of emission that is aligned nearly east-west. On larger scales, the pulsar candidate is centered on an arcminute-long ridge of fainter emission that is also oriented in roughly the east-west direction. The pulsar candidate is located about $0.9'$ from our eyeball estimate of the geometric center of the remnant, which is indicated by the plus sign on Fig. 3.

Within a radius of 2.5 pixels ($1.23''$) centered on the position of the pulsar candidate we obtain a total of 3326 ACIS-S events for a count rate of 0.0773 ± 0.0014 s^{-1}. Background, both instrumental and from the rest of G292.0+1.8 itself, was sufficiently small in this aperture to be neglected. An absorbed power-law provided an acceptable fit to the *Chandra* data. Numerical values from the fits are given in Table 1 and the spectrum is plotted in Fig. 2. Including an additional black body thermal component (with best-fitted $kT_{\rm BB} = 0.16$ keV) provided an improved spectral fit that resulted in a flatter power-law spectral index ($\alpha = 1.66$) and more absorption ($N_{\rm H} = 3.8 \times 10^{21}$ H atoms cm^{-2}). However, according to the F-test, the reduction in χ^2 with the addition of this component was not statistically significant. The unabsorbed fluxes of the pulsar candidate, based on the pure power-law fits, are 6.9×10^{-13} ergs cm^{-2} s^{-1} (0.2–4 keV band) and 4.8×10^{-13} ergs cm^{-2} s^{-1} (2–8 kev band).

Detection of pulsed emission would clearly confirm the pulsar hypothesis. Unfortunately the low time resolution implicit in the ACIS Timed Exposure mode makes detection of rapid pulsations impossible. We searched unsuccessfully for pulsed emission from the vicinity of the pulsar candidate in the *ROSAT* HRI and PSPC data. In neither data set was the candidate detected as a resolved source, due to the poorer angular resolution of these instruments, the strong soft thermal X-ray emission, and the low statistical signal. In addition there have been no reports of pulsed X-ray emission from G292.0+1.8 from either ASCA or RXTE.

The spectrum of the diffuse nebula is significantly contaminated by the remnant's soft thermal emission within annular apertures even rather close to the pulsar candidate. For example, the aperture extending over $3'' - 5''$ unmistakeably shows soft thermal emission (i.e., prominent lines of O, Ne, and Mg), which introduces significant uncertainty into the derived spectral properties of the hard, diffuse nebula. Nevertheless out to a radius of $20''$ we were able to confirm that the spectrum above 3 keV is a power law with photon index in the range $\alpha_p = 1.7 - 2.0$. Because of the thermal contamination it was not possible to determine if the photon index of the nebular emission steepened with radius. Such an effect has been seen in other Crab-like SNRs with *Chandra* (e.g., G21.5−0.9; Slane et al. 2000) and is expected for an extended synchrotron nebula powered by a central pulsar.

The total X-ray flux of the diffuse nebula is an important observable that we estimated in the following manner. In the 4–8 keV band the radial profile of the diffuse nebula centered on the pulsar candidate fell roughly as an exponential with radius. The profile was summed out to the radius where the emission was twice the background level, which yielded a total count rate of 0.145 s^{-1}. For comparison the pulsar candidate count rate in the same energy band is only 0.0074 s^{-1}, while at the other extreme, the total background subtracted rate from G292.0+1.8 is 0.2188 s^{-1}. Thus the diffuse nebula accounts for 66% of the total 4–8 kev flux from the remnant. We assumed the nebular spectral parameters to be the same as those of the pulsar candidate in order to convert the band-limited count rate to fluxes. The estimated nebular spectrum is shown in Fig. 2 (as the middle curve). Our estimates of the unabsorbed fluxes from the nebula are 1.5×10^{-11} ergs cm^{-2} s^{-1} (0.2–4 keV band) and 1×10^{-11} ergs cm^{-2} s^{-1} (2–8 kev band). The hard band flux would increase by only about 10% if we assume that the nebula's spectrum is steeper, with $\alpha_p = 2.1$ like the Crab. The increase in the soft band flux in this case would be much larger, about a factor of 2.

4. Discussion and Results

We have presented evidence for a point-like source embedded in a diffuse nebula, both of which exhibit featureless hard X-ray emission and are spatially coincident with a flat-spectrum radio source in the SNR G292.0+1.8. These features are the classic signatures of a young rapidly-rotating pulsar and its associated synchrotron, or pulsar wind, nebula (PWN). We attribute the power-law spectral form of the pulsar candidate to nonthermal synchrotron emission from electrons accelerated by the high surface field near the magnetic poles of the neutron star. Although this is the dominant component, our spectral fits do allow for significant cool ($T \sim 2 \times 10^6$ K) thermal blackbody emission, covering of order 5% of the neutron star's surface area.

The spin-down energy loss rate of the pulsar can be estimated using the established correlation between this quantity and the nebular X-ray luminosity (e.g., Seward & Wang 1988). From our flux estimate we obtain an unabsorbed luminosity (0.2–4 keV band) of $L_X = 4 \times 10^{34} D^2_{4.8\,\rm kpc}$ ergs s^{-1}, assuming the Hi absorption distance of 4.8 kpc (Saken, Fesen, & Shull 1992), which implies only a modest spin-down energy loss rate of $\dot{E} \sim 7 \times 10^{36}$ ergs s^{-1}. Another estimate of the spin-down energy loss rate can be derived from the radio luminosity of the PWN. Braun et al. (1986) quote a flux density of 6.2 Jy at 843 MHz for the bright ridge of radio emission in G292.0+1.8 that coincides with the *Chandra* point source. Assuming this emission arises entirely from the PWN and integrating the radio spectrum from 10^7 Hz to 10^{11} HZ with a spectral index of -0.4 yields a radio luminosity of $L_R = 4.2 \times 10^{33}$ erg s^{-1}. On average, for PWN in young supernova remnants $\dot{E} \approx 3.3 \times 10^3\, L_R$ (Frail & Scharringhausen 1997), so we find a very similar value of $\dot{E} \sim 1.4 \times 10^{37}$ ergs s^{-1}.

Based on the lower X-ray–derived $\dot{E}$ estimate, then for a braking index $n = 3$, and assuming that the current spin period P is much longer than the initial value, the remnant age implies $P \sim 280$ ms and a spin-down rate $\dot{P} \sim 3 \times 10^{-12}$ s s^{-1}. This corresponds to a surface magnetic field strength $B \sim 10^{13}$ G, which is quite large. This value is reduced if we relax the constraint that $P \gg P_0$. We note that there are considerable uncertainties in this estimate, including the relationship between L_x (or L_R) and $\dot{E}$ (see, e.g., Chevalier 2000). Clearly discovery of the pulsed emission from the new pulsar candidate is of highest priority. Observations optimized for fast timing using the HRC on *Chandra* have been approved for observation in cycle 2 and will be carried out soon.

The pulsar candidate is not directly at the geometric center of the remnant, suggesting that it has moved since birth. Its implied transverse speed of $\sim 770 (D/4.8\,\mathrm{kpc})(t/1600\,\mathrm{yr})^{-1}\,\mathrm{km\,s^{-1}}$ is in good agreement, given our uncertainties, with the mean birth velocity of pulsars of $450 \pm 90\,\mathrm{km\,s^{-1}}$ (Lyne & Lorimer 1994). Concerning the uncertainties in our velocity estimate we note that it is likely that the blast wave has expanded more slowly toward the southeast in G292.0+1.8. This is where the optical emission is most intense and thus where the density of the ambient interstellar medium should be highest. If true this would shift the true center of the remnant toward the southeast and thereby reduce the implied transverse velocity of the pulsar candidate. We note that there is no evidence in the X-ray band for a bow shock preceding the pulsar candidate in this, or any, direction.

To summarize, the *Chandra* data reveal the effects of a central pulsar on three spatial scales in G292.0+1.8: an unresolved source (the pulsar candidate itself); a compact resolved region of X-ray emission surrounding the point source and an extended pulsar wind nebula. The compact emission near the pulsar (see insert to Fig. 3) shows a symmetric component, $\sim 1.5''$ (0.035 pc) in size, as well as an elongated ridge of emission covering roughly $3'' \times 10''$ (0.07×0.23 pc). Such compact, but resolved, components have been seen by *Chandra* near the central compact objects in other known pulsar-wind nebula, specifically the Crab (Weisskopf et al. 2000) and G21.5−0.9 (Slane et al. 2000). These structures, on scales of tenths of parsecs, have been interpreted as arising from the pulsar wind termination shock (e.g., Rees & Gunn 1974, Kennel & Coroniti 1984). On larger scales the triangular morphology of the extended pulsar wind nebula in G292.0+1.8 bears considerable similarity as well to the overall shape of the Crab Nebula. The physical sizes are similar as well. The bright portion of the nebula in G292.0+1.8 between the light and dark contours in Fig. 3 is roughly 1 pc across, which is just about the same size as the long extent of the so-called X-ray torus in the Crab Nebula.

During its first year of operation *Chandra* has discovered point-like sources within the two youngest Galactic oxygen-rich supernova remnants (Cas A and G292.0+1.8) that are likely the compact remnants of these SN explosions. The compact object in Cas A remains mysterious (e.g., Pavlov et al. 2000), while the one in G292.0+1.8 appears to have characteristics that are consistent with a young rapidly-rotating pulsar like the Crab pulsar. Interestingly enough Cas A and G292.0+1.8 also differ in the properties of their X-ray emitting ejecta. Cas A is dominated by Si- and Fe-rich ejecta that were likely produced by explosive O- and Si-burning (Hughes et al. 2000). In G292.0+1.8, on the other hand, we have been unable to find evidence for either of these particular types of nucleosynthetic yields, while the most common ejecta features are rich in O, Ne, and Mg. Further study should reveal whether these differences in the X-ray emitting ejecta are due to an evolutionary or age effect or whether they signal more fundamental differences in the stellar progenitors. Such studies using *Chandra* will offer us a new window on the connection between compact objects and the SN progenitors that form them.

This research has made use of the SIMBAD Astronomical Database maintained by the Centre de Données astronomiques de Strasbourg. Financial support was provided by NASA contracts NAS8-38252 (PSU) and NAS8-39073 (SAO), NASA grant NAG5-9281 (SAO), and *Chandra* grant GO0-1035X (Rutgers).

REFERENCES

Bautz, M. W., et al. 1998, in Proc. SPIE Vol 3444, X-ray Optics, Instruments, and Missions, ed. R. B. Hoover & A. B. Walker, 210.

Chevalier, R. A. 2000, ApJ, 539, L45

Braun, R., Goss, W. M., Caswell, J. L., & Roger, R. S. 1986, A&A, 162, 259

Frail, D. A., & Scharringhausen, B. R. 1997, ApJ, 480, 364

Garmire, G. P., et al. 1992, AIAA Space Program and Technologies Conference, Huntsville, AL

Goss, W. M., Shaver, P. A., Zealey, W. J., Murdin, P., & Clark, D. H. 1979, MNRAS, 188, 357

Hughes, J. P., Rakowski, C. E., Burrows, D. N., & Slane, P. O. 2000, ApJ, 528, L109

Kennel, C. F., & Coroniti, F. V. 1984, ApJ, 283, 694

Lyne, A. G., & Lorimer, D. R. 1994, Nature, 369, 127

Milne, D. K. 1969, Australian J. Phys., 22, 613

Murdin, P., & Clark, D. H. 1979, MNRAS, 189, 501

Pavlov, G. G., Zavlin, V. E., Aschenbach, B., Trümper, J., & Sanwal, D. 2000, ApJ, 531, L53

Rees, M. J., & Gunn, J. E. 1974, MNRAS, 167, 1

Seward, F. D., & Wang, Z. R. 1988, ApJ, 332, 199

Shaver, P. A., & Goss, W. M. 1970, Australian J. Phys., Astr. Suppl., 14, 133

Saken, J. M., Fesen, R. A., & Shull, J. M. 1992, ApJS, 81, 715

Slane, P., Chen, Y., Schulz, N. S., Seward, F. D., Hughes, J. P., & Gaensler, B. M. 2000, ApJ, 533, L29

Torii, K., Tsunemi, H., & Slane, P. 1998, in IAU Symp. 188 The Hot Universe, ed. K. Koyama, S. Kitamoto, & M. Itoh (Dordrecht: Kluwer), 258

Wallace, B., & Gaensler, B. 1997, poster presented at the Minnesota SNR Workshop, March 23-26, 1997

Weisskopf, M. C., et al. 2000, ApJ, 536, L81

This preprint was prepared with the AAS LaTeX macros v4.0.

Fig. 1.— *Chandra* ACIS-S X-ray images of G292.0+1.8 in soft (left: 0.6–2 keV) and hard (right: 2–7 keV) X-ray bands. The hard band clearly shows a diffuse, plerionic nebula containing a central point-like source. The grayscale display for the hard band has been adjusted so that the diffuse emission can be seen clearly, which has "burned in" the point-like source causing it to appear extended. Note that the point source can also be seen in the soft band image, where it appears essentially unresolved.

Fig. 2.— ACIS-S X-ray spectrum of the entire G292.0+1.8 supernova remnant (data points at top), the estimated power-law model for the diffuse nebula (middle curve), and the hard point source ("pulsar candidate") with best-fit power-law model (data points and curve at bottom). Above 4 keV the diffuse nebula accounts for 66% of the total flux from G292.0+1.8. The pulsar candidate spectrum extracted from circular region 2.5 pixels (1.23″) in radius was rebinned to 25 counts per channel before fitting to ensure appropriate Gaussian errors for χ^2 fitting.

Fig. 3.— *Chandra* ACIS-S 4–8 keV band X-ray image of the pulsar wind nebula in G292.0+1.8. The diffuse emission was adaptively smoothed to an approximate signal-to-noise ratio of 10, while the unresolved sources were smoothed using a single gaussian with $\sigma = 0.5''$. The contour levels are plotted at values of 0.0173, 0.0254, 0.0372, 0.0547, 0.0802, 0.118, 0.173, 0.619, 2.22 cts s^{-1} $arcmin^{-2}$. The insert shows the raw 4–8 keV band data in the immediate vicinity of the pulsar candidate in unblocked pixels (i.e., $0.492'' \times 0.492''$). This image is centered on the pulsar candidate and the axis labels are in units of arcseconds as indicated. The brightest pixel contains 45 detected events. Note the roughly east-west extension of the central X-ray emission on both large and small spatial scales. The plus sign in the main image panel marks the approximate center of the soft thermal emission of the remnant.

Table 1. Power-law Spectral Model Fits for Pulsar Candidate

Parameter	Value and Uncertainty (1 σ)
$N_{\rm H}$ (H atoms cm^{-2})	$3.17 \pm 0.15 \times 10^{21}$
$\alpha_{\rm P}$	1.72 ± 0.05
$F_{\rm E}(1\,{\rm keV})$ (photon s^{-1} cm^{-2} keV^{-1})	$1.44 \pm 0.07 \times 10^{-4}$
χ^2/d.o.f	116.1/102

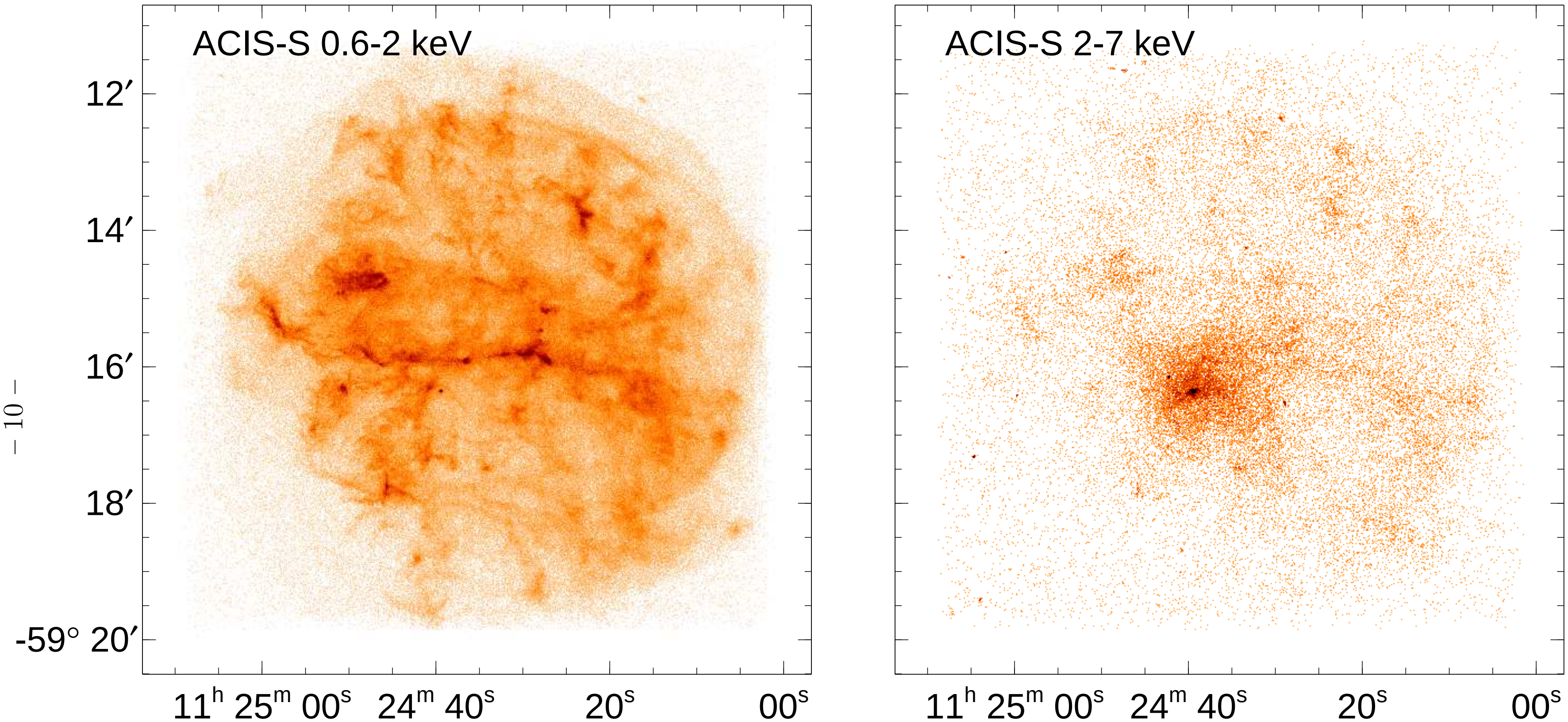
ACIS-S 0.6-2 keV
ACIS-S 2-7 keV
12′
14′
16′
18′
-59° 20′
11h 25m 00s
24m 40s
20s
00s

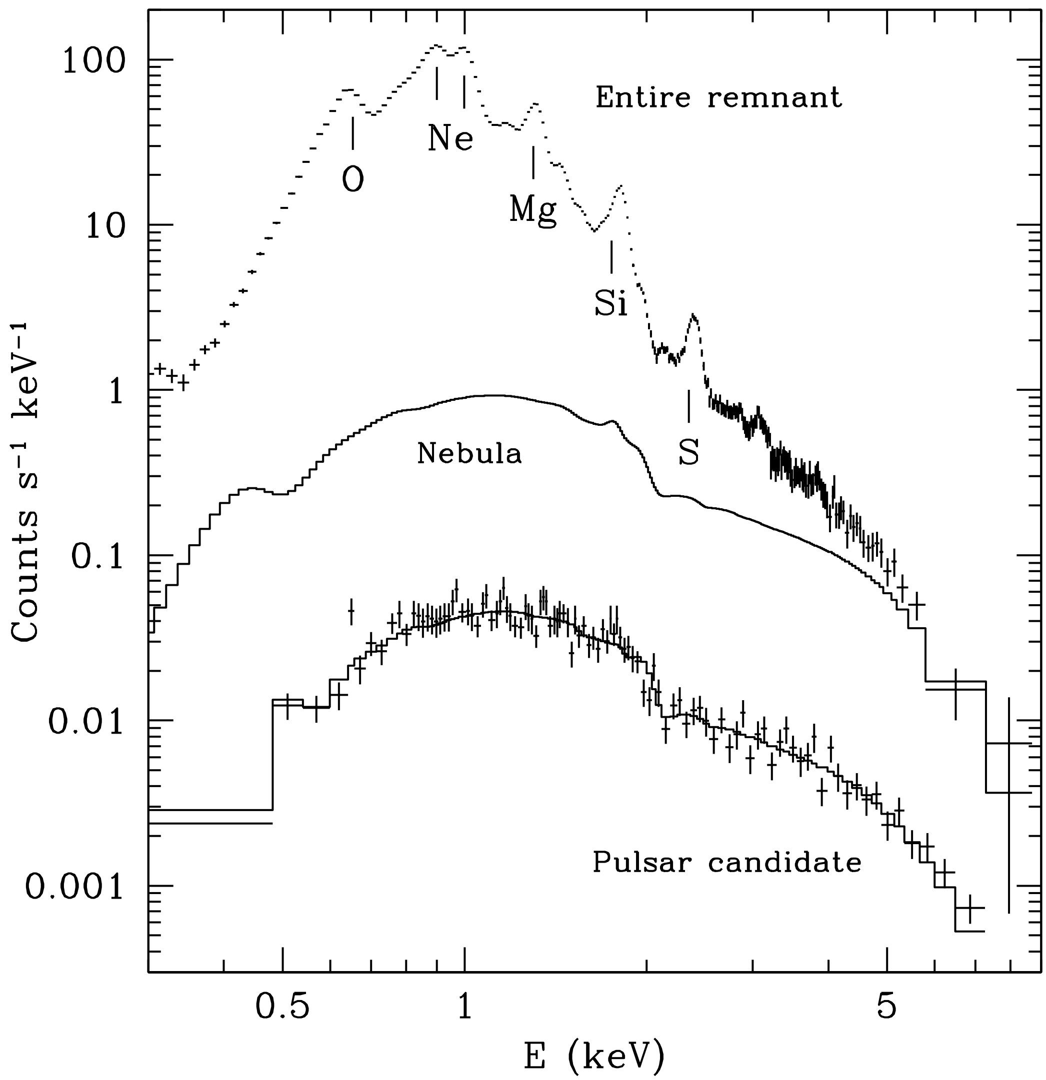
Entire remnant
O
Ne
Mg
Si
S
Nebula
Pulsar candidate
100
10
1
0.1
0.01
0.001
Counts s^{-1} keV^{-1}
0.5
1
5
E (keV)

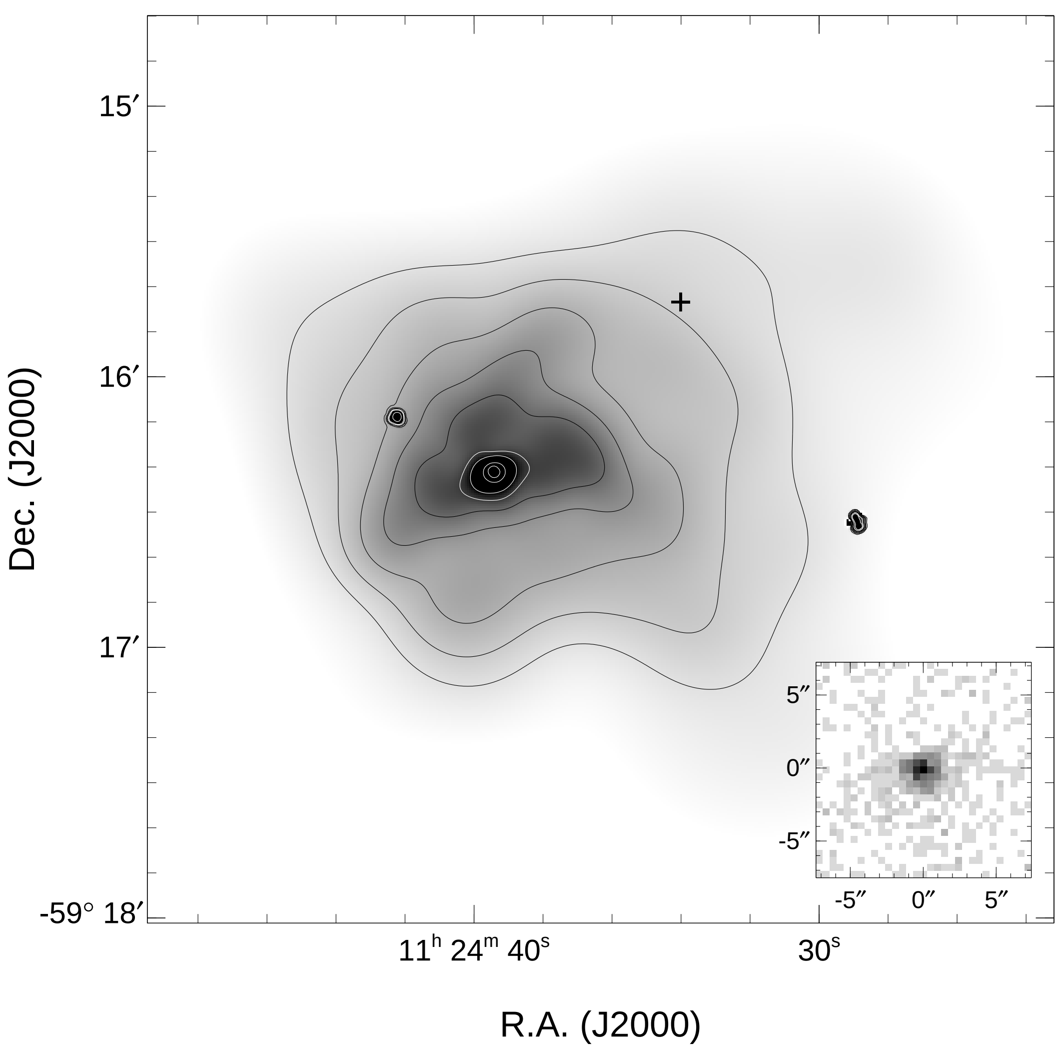
15′
16′
17′
-59° 18′
Dec. (J2000)
11h 24m 40s
30s
R.A. (J2000)
5″
0″
-5″
-5″
0″
5″